Biomimetic Synthesis

DOI: 10.1002/anie.201203483

DNA/Polymeric Micelle Self-Assembly Mimicking Chromatin Compaction**

*Kaka Zhang, Ming Jiang, and Daoyong Chen**

Through self-assembly, a large variety of nanomaterials have been fabricated, which are useful in many applied and research fields.[1–6] However, broader development of nanoscience and nanotechnology requires more complex nanostructures whose fabrication requires precise control of morphology, structural parameters, and distributions of components within the nanomaterials, which remains a great challenge for nanotechnology. Nature is masterful at building nanostructures with great complexity by precisely controlling multi-stage self-assembly processes. One example is the self-assembly of genomic DNA and histone octamers into chromatin in eukaryotic cells. Histone octamers are disc-shaped nanostructures with positively-charged binding sites specifically distributed on the edge of the disc.[7] In the first stage, a DNA chain organizes histone octamers into a beads-on-a-string structure (10 nm chromatin fiber); the bead is a nucleosome composed of one DNA segment wrapping around the edge of one histone octamer, and between neighboring beads is a short DNA linker.[8,9] In the second stage, histone octamers that are preorganized on the 10 nm chromatin fiber, self-assemble further in a zigzag manner into the 30 nm chromatin fiber with a two-start helical structure.[10,11] Histone octamers do not self-assemble into the 30 nm fiber until they are preorganized by the first stage of self-assembly; the first stage self-assembly initiates the second stage self-assembly. Inspired by such efficient self-assembly processes from nature, a number of DNA/sphere systems were studied;[12,13] artificial nanospheres were used in the place of histone octamers. Computer simulation of the interaction between a polyelectrolyte with long DNA-like semi-flexible chains and the spheres with a uniform oppositely-charged surface reveals that the beads-on-a-string structure, similar to the 10 nm chromatin fiber, is the thermodynamic favored structure. However, experimentally, other kinetically trapped structures were inevitably produced in the reported systems because the DNA/sphere interactions were relatively strong.

Herein, we prepared thermodynamically optimal structures of a DNA/artificial particle complex by controlling the interaction between DNA and the particles. We selected the block-copolymer micelles with an inert shell and a positively charged core to interact with DNA (Figure 1 A); the interaction strength between DNA and the core can be continuously adjusted by the pH value of the medium. It was found that under certain conditions the strings (that are similar to the 10 nm chromatin fibers in both morphology and structure) formed exclusively. Under such conditions, only the thermodynamically favored beads-on-a-string structure can persist, while any kinetically trapped structures cannot. When monodisperse DNA was used, the strings formed were monodisperse, and the earlier-formed long strings evolved to shorter, but also monodisperse, strings; the different strings formed and evolved in a similar manner. Then, in a second stage, the micelles preorganized in the beads-on-a-string structure self-assembled along the strings into core–shell structured solenoidal nanofibers. The preorganization induced and guided the second stage of self-assembly. When monodisperse DNAs are used, the resulting nanostructures are monodisperse. This self-assembly process can be used for synthesis of monodisperse one-dimensional nanostructures with controlled dimensions and various compositions.

Poly(ethylene glycol)$_{113}$-*b*-poly(4-vinylpyridine)$_{58}$ (PEG$_{113}$-*b*-P4VP$_{58}$, subscripts represent the average degrees of polymerization; $M_w/M_n = 1.20$) micelles were prepared in a water/methanol (4:1, *v*/*v*) mixture (see Supporting Information, Text S1). The micelles were monodisperse in size with an average hydrodynamic radius $\langle R_h \rangle$ of 16.0 nm, a polydispersity index (PDI) of 0.05, and an average molecular weight of 1.74×10^6 g mol^{-1}, based on light scattering (LS) measurements. In the TEM images, the micelles are monodisperse with a size of 17.5 ± 1.5 nm (Figure 1 B). The micelles shown have PEG as the shell and P4VP as the core.

An aqueous solution of monodisperse linear double-stranded DNA 5427 bp long (L5427) at 25 °C was added to the micelles in the water/methanol mixture to give a DNA/micelle mass ratio of 1:20. The solution had a pH value of 6.6 in the presence of carbon dioxide (see Experimental Section), which provided the proper strength for the electrostatic interaction between DNA and the micelles (Supporting Information, Text S2). After 0.5 hours incubation, strings with a beads-on-a-string structure formed exclusively (Figure 1 C). These strings have a linear structure without any branches, indicating that each string is composed of a single L5427 DNA chain, as detailed below. For each string, the beads were very similar in shape and size to the micelles. Between neighboring beads was a linker, which appears to be a short DNA segment. Additionally, the strings were shown to

[*] K. Zhang, Prof. M. Jiang, Prof. D. Chen
The State Key Laboratory of Molecular Engineering of Polymers and Department of Macromolecular Science, Fudan University
Handan Road 220, Shanghai 200433 (P.R. China)
E-mail: chendy@fudan.edu.cn

[**] We are grateful for the financial support of NSFC (50825303, 91127030 and 30890140), the Ministry of Science and Technology of China (2009CB930400, 2011CB932503), the Shanghai Committee of Science and Technology, China (11XD1400400), and the Innovative Team of Ministry of Education of China (IRT0911).

Supporting information for this article is available on the WWW under http://dx.doi.org/10.1002/anie.201203483.

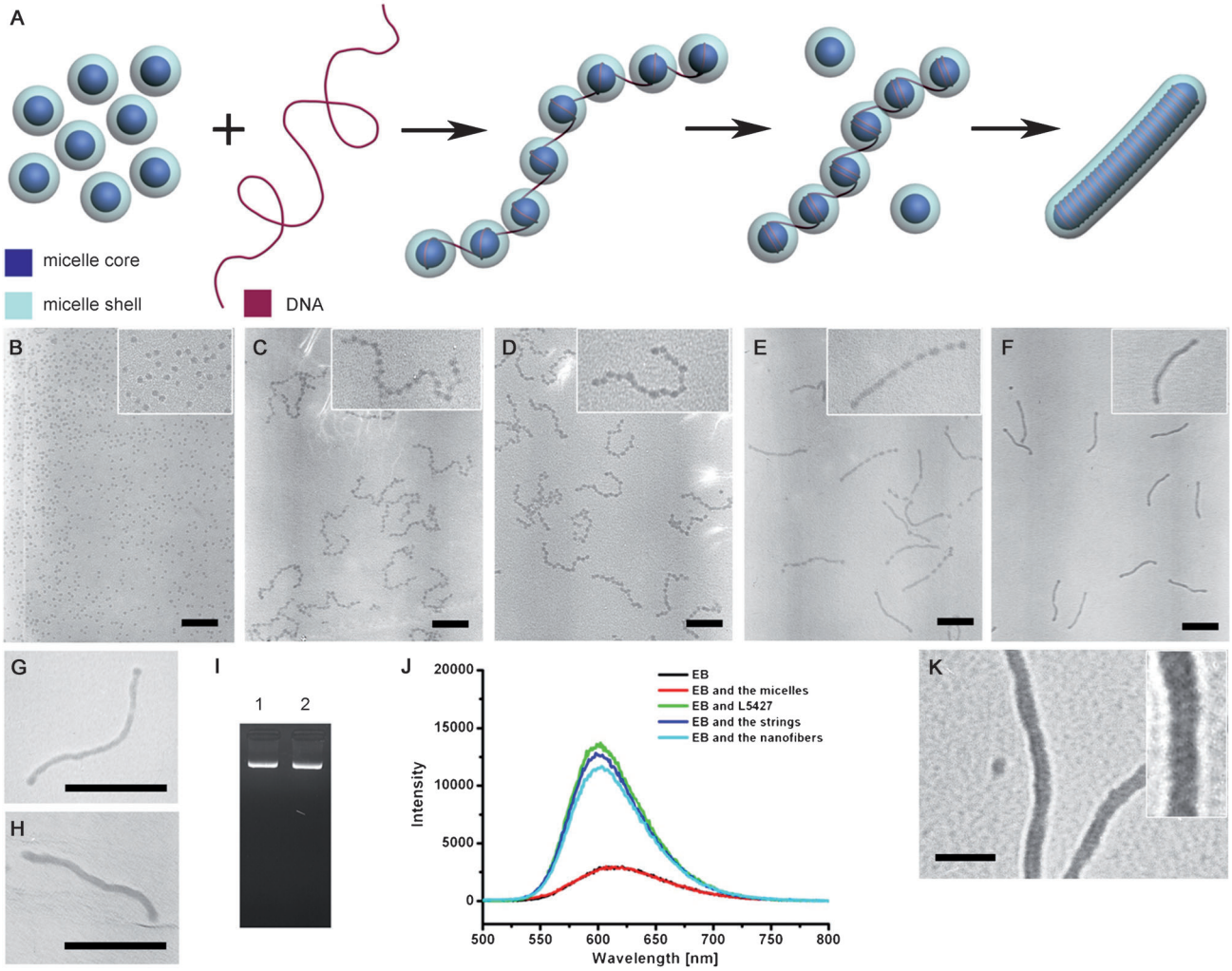

Figure 1. Self-assembly of linear DNA and the core-shell micelles. A) A schematic representation of the assembly process. B–F) TEM images of PEG_{113}-*b*-$P4VP_{58}$ micelles (B), and the nanostructures formed in the mixture of DNA (L5427) and the micelles after incubation for 0.5 h (C), 10 h (D), 32 h (E) and $\geq$48 h (F). G, H) TEM images of an unstained nanofiber (G) and a phosphotungstic acid-stained nanofiber (H). I) Gel electrophoresis of L5427 DNA recovered from the strings (lane 1) and pristine L5427 (lane 2, a control). J) Fluorescent spectra of ethidium bromide (EB) mixed with micelles alone, DNA alone, self-assembled strings, and nanofibers (excited at 482 nm). The number ratio of EB/DNA base pairs is 1:6. K) TEM image of the nanofibers stained by aniline-coated gold clusters, which selectively bind DNA. Insets: higher magnification. Scale bars in B–H) represent 200 nm, and that in K) 50 nm.

be monodisperse. The average number of beads per string was 22 ± 1 and the number-average length (L_n) of the strings was 587 nm ($L_w/L_n = 1.004$, L_w represents weight-average length). LS measurements gave an $\langle R_h \rangle$ of 55.8 nm with a PDI as small as 0.02 and an $\langle R_g \rangle / \langle R_h \rangle$ ratio of 1.7 (where $\langle R_g \rangle$ = average gyration radius), confirming the size, monodispersity, and linear structure of the strings. The length of the strings (587 nm) was remarkably shorter than the contour length of L5427 (1845 nm). Gel electrophoresis of L5427 recovered from the strings ruled out the possibility that L5427 experienced breakage during self-assembly (Figure 1 I and Supporting Information, Text S3). This shows that, L5427 was compacted in the beads-on-a-string structures, and the compaction ratio was 3.1.

After 10 hours incubation, all the monodisperse 587 nm long strings evolved into shorter (434 nm), but still monodisperse, strings containing 16 ± 1 micelles each ($L_w/L_n =$ 1.008 and the compaction ratio is 4.3; Figure 1 D). These measurements strongly suggest that, in each of the strings, a DNA chain organizes the micelles into a string by wrapping around the individual micelles (Figure 1 A), because only this interaction could explain the precise structure and evolution observed. The structure of DNA wrapped around the individual micelles was confirmed by TEM images, as described below. Therefore, the strings are very similar to the 10 nm chromatin fibers in both morphology and structure. According to computer simulations,[12] these strings are the thermodynamically optimal product of the interaction between DNA and the micelles. The fact that the strings were formed exclusively, indicates that any kinetically trapped structures were unstable under the conditions used. Actually, the 587 nm strings are a locally optimal product, so they will further evolve to 434 nm strings under the identical conditions. The formation of 434 nm strings takes longer

because more conformational adjustments of both the DNA and the micelles are needed.

After longer incubation, the second stage of the DNA/micelle self-assembly occured, the strings fused into monodisperse nanofibers (Figure 1F). An intermediate structure between the strings and the nanofibers was also observed after 32 hours incubation (Figure 1E). The final nanofibers had an L_n of 232 nm ($L_w/L_n = 1.003$) and a compaction ratio of 8.0. The respective values of $\langle R_h \rangle$, PDI, and $\langle R_g \rangle/\langle R_h \rangle$ of the nanofibers were determined by LS to be 62.3 nm, 0.03, and 1.8, respectively, consistent with the size, monodispersity, and cylindrical morphology observed by TEM. It was also confirmed, by TEM observations of freeze-dried samples of the strings and the nanofibers, that solvent evaporation during drying the TEM samples has no considerable effect on their morphologies (Supporting Information, Figure S1). Within TEM images, the PEG shell of the nanofibers was invisible (Figure 1G) but became visible after staining with phosphotungstic acid (Figure 1H), as revealed by the difference between the widths of the stained nanofibers (19.1 nm) and the unstained nanofibers (16.0 nm). It was noticed that, in the TEM images, no difference in contrast can be seen in the unstained nanofibers. This indicates that the P4VP cores fused together in the nanofibers, otherwise the low contrast PEG domains sandwiched between the relatively high contrast P4VP domains would have been seen. Circular dichroism spectra of the nanostructures revealed that the DNA chains of both the strings and the nanofibers are still in a B-form (Supporting Information, Figure S2). Experiments using ethidium bromide as a probe demonstrated that 92% of the binding sites of the DNA in the strings and 84% in the nanofibers are still accessible to intercalation by ethidium bromide (Figure 1J and Supporting Information, Text S4). Therefore, the DNA chains are located on the surface rather than encapsulated in the P4VP cores; it has been shown that DNA chains encapsulated by an interacting polymer are inaccessible to ethidium bromide binding.[14] TEM images of the nanofibers stained with positively charged aniline-coated gold clusters, which selectively stain DNA,[15] reveal that DNA wraps around P4VP cylindrical cores like a solenoid (Figure 1K and Supporting Information, Text S5). The results of these TEM observations and the ethidium bromide experiments confirm that DNA wraps around the micelles to form the strings. To our knowledge, synthesis of solenoidal nanofibers has not been previously reported. The pitch of the DNA solenoid is 5.4 nm (Figure 1K), which is close to the calculated value of 6.3 nm (Supporting Information, Text S6). Similar to the self-assembly of 10 nm chromatin fibers, in the second stage of chromatin compaction, the self-assembly of the micelles on the strings resulted from their preorganization; in the absence of DNA, the micelles disperse individually in the solution. The cores of the preorganized micelles in a string, driven by hydrophobic interaction between the neighboring P4VP cores and the interaction between the P4VP cores and the linker, overcome the shell–shell repulsion between the neighboring micelles to fuse together; the preorganization of the micelles induced and guided the second stage of self-assembly. It is possible that core–core fusion requires deformation of the micelles and redistribution of the PEG chains, which necessitates flexibility of the micelles;[6] this flexibility results from the addition of methanol to the solution.

The DNA/micelle self-assembly can be used for tailored synthesis of the solenoidal nanofibers of different lengths. The monodisperse nanofibers of 113 nm, 232 nm, and 402 nm lengths were prepared from monodisperse linear DNA of 2686, 5427, and 8592 bp, respectively (M1–M3 in Table 1, Figure 2A–C; see also Supporting Information, Figure S3). The diameter can also be changed; the diameter of the nanofibers prepared from PEG_{113}-*b*-$P4VP_{58}$ micelles is 16 nm (M1–M3), while that from PEG_{113}-*b*-$P4VP_{101}$ micelles is 29.3 nm (P1 in Table 1, Figure 2D). The nanofibers with poly(*N*,*N*-dimethylacrylamide) (PDMA) as the shell were obtained through self-assembly of DNA L2000 with $PDMA_{52}$-*b*-$P4VP_{62}$ micelles under identical conditions (P2 in Table 1, Figure 2E). P1 and P2 nanofibers are polydisperse since polydisperse DNAs were used. Additionally, DNA can organize PEG_{113}-*b*-$P4VP_{58}$ micelles and PEG_{113}-*b*-$P4VP_{101}$ micelles together into binary strings (Figure 2F, polydisperse DNA was used). Hydrolysis of tetramethoxysilane within M2 (232 nm long) and M3 (402 nm long) solenoidal nanofibers produced monodisperse hybrid nanofibers of 307 nm and 432 nm, respectively (Figure 2G,H, Supporting Information, Text S7);[16] the solenoidal conformation of the DNA chains in M2 and M3 nanofibers makes this elongation possible. The self-assembly leads to solenoidal nanofibers with tailored dimensions, varied compositions, and a high linear density (16 PEG_{113}-*b*-$P4VP_{58}$ chains/nm for M2 nanofibers based on LS measurements; the linear density is comparable to that of worm-like micelles).[17–19] The nanofibers were also prepared on a gram scale; grams of the nanofibers were prepared from 500 mL of a solution of PEG_{113}-*b*-$P4VP_{58}$ micelles (4.0 mg mL^{-1}) with commercially available DNA L20k (a polydisperse DNA averaging 20 kilobases; 0.2 mg mL^{-1}; Figure 3). The nanofibers in Figure 3 were silicified so that the outline of each nanofiber in a stack of the nanofibers can be seen clearly.

In conclusion, when monodisperse DNA was used, the assemblies of DNA and polymeric micelles evolved from the quickly formed, longer beads-on-a-string structure to shorter more-condensed strings, and finally to monodisperse solenoidal nanofibers. The unique features of this self-assembly

Table 1: Tailored synthesis of nanofibers.

Entry[a]	DNA[b]	Block copolymer	Diameter [nm]	Length [nm] (L_w/L_n)	Compaction ratio
M1	L2686	PEG_{113}-*b*-$P4VP_{58}$	16.0 ± 2.0	113 (1.002)	8.1
M2	L5427	PEG_{113}-*b*-$P4VP_{58}$	16.0 ± 1.8	232 (1.003)	8.0
M3	L8592	PEG_{113}-*b*-$P4VP_{58}$	16.7 ± 1.4	402 (1.007)	7.3
P1	L2000	PEG_{113}-*b*-$P4VP_{101}$	29.3 ± 2.5	-	-
P2	L2000	$PDMA_{52}$-*b*-$P4VP_{62}$	17.3 ± 1.8	-	-

[a] M1–M3: monodisperse DNAs were used. P1 and P2: polydisperse DNAs were used. [b] The number represents the length (bp) of the linear DNA.

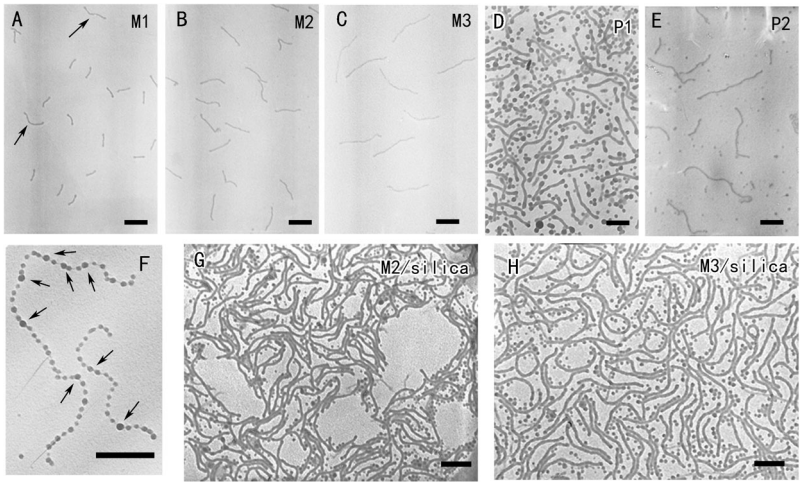

Figure 2. Tailored synthesis of nanofibers. A–C) TEM images of the monodisperse nanofibers prepared from A) L2686, B) L5427, and C) L8592 (see M1–M3 in Table 1) The arrows in (A) point to a head-to-head connection between two 113 nm fibers. D, E) TEM images of thicker nanofibers and nanofibers with a PDMA shell (see P1 and P2 in Table 1). F) TEM image of the binary nanostrings (arrows indicate the PEG_{113}-*b*-$P4VP_{101}$ micelles). G, H) TEM images of hybrid nanofibers prepared by hybridizing M2 nanofibers and M3 nanofibers, respectively. Scale bars = 200 nm.

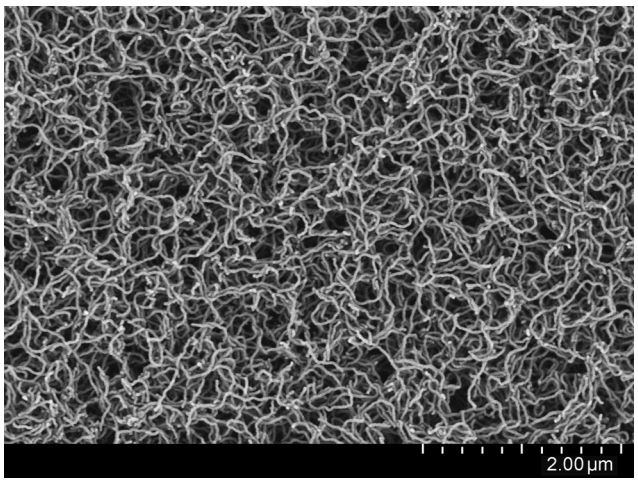

Figure 3. SEM image of the silicified nanofibers prepared from L20k DNA (0.2 mg mL^{-1}) and PEG_{113}-*b*-$P4VP_{58}$ micelles (4.0 mg mL^{-1}).

process are: 1) Each of the nanostructures is the thermodynamically optimal structure of the corresponding assembly stage; 2) From the beginning, the different nanostructures formed and evolved in a similar manner and at a similar step. These two features reveal that the pathway for nanostructure formation and evolution is prescribed thermodynamically. Compared with reported artificial self-assembly systems, to our knowledge, this precision in nanostructure formation and evolution is unprecedented. Additionally, from the viewpoint of chemical synthesis, the present study has several advantages: 1) There are no byproducts (e.g. kinetically trapped nanostructures) formed during self-assembly; 2) Monodisperse nanofibers can be prepared when monodisperse DNAs are used; 3) The dimensions and compositions of the nanofibers can be tailored to different specifications; 4) This method allows large-scale synthesis. These advantages make the DNA/micelle self-assembly described herein very promising for addressing both theoretical and practical problems.

Experimental Section

PEG_{113}-*b*-$P4VP_{58}$ micelles were prepared in a water/methanol (4:1, *v*/*v*) mixture by adding carbon dioxide saturated water into a PEG-*b*-P4VP (2.0 mg mL^{-1}) methanol solution (methanol is a common solvent for both PEG and P4VP, and water is a selective solvent for PEG). Carbon dioxide was used to adjust the pH value without introducing salts into the suspension; our study shows that salt affects the interaction considerably because the interaction between DNA and the micelles is electrostatic (Supporting Information, Text S2). For the self-assembly of DNA and micelles, typically, 1 mL DNA solution in deionized water (0.2 mg mL^{-1}) was added into 10 mL of the micelle solution (0.4 mg mL^{-1}) over 5 min. In the final mixture, the mass ratio of DNA to the micelles is 1:20 (the number of the micelles, in the mixture, is slightly larger than that required to form the beads-on-a-string structure in which DNA wraps one turn around each micelle).

Received: May 6, 2012
Revised: June 12, 2012
Published online: July 24, 2012

Keywords: biomimetic synthesis · DNA · micelles · nanomaterials · self-assembly

[1] L. F. Zhang, A. Eisenberg, *Science* **1995**, *268*, 1728.
[2] D. Y. Yan, Y. F. Zhou, J. Hou, *Science* **2004**, *303*, 65.
[3] P. Jonkheijm, P. van der Schoot, A. Schenning, E. W. Meijer, *Science* **2006**, *313*, 80.
[4] X. S. Wang, G. Guerin, H. Wang, Y. S. Wang, I. Manners, M. A. Winnik, *Science* **2007**, *317*, 644.
[5] H. G. Cui, Z. Y. Chen, S. Zhong, K. L. Wooley, D. J. Pochan, *Science* **2007**, *317*, 647.
[6] K. Zhang, M. Jiang, D. Chen, *Prog. Polym. Sci.* **2012**, *37*, 445.
[7] K. Luger, A. W. Mader, R. K. Richmond, D. F. Sargent, T. J. Richmond, *Nature* **1997**, *389*, 251.
[8] A. L. Olins, D. E. Olins, *Science* **1974**, *183*, 330.
[9] R. D. Kornberg, *Science* **1974**, *184*, 868.
[10] B. Dorigo, T. Schalch, A. Kulangara, S. Duda, R. R. Schroeder, T. J. Richmond, *Science* **2004**, *306*, 1571.
[11] T. Schalch, S. Duda, D. F. Sargent, T. J. Richmond, *Nature* **2005**, *436*, 138.
[12] T. T. Nguyen, B. I. Shklovskii, *J. Chem. Phys.* **2001**, *114*, 5905.
[13] A. A. Zinchenko, K. Yoshikawa, D. Baigl, *Phys. Rev. Lett.* **2005**, *95*, 228101.
[14] W. Chen, N. J. Turro, D. A. Tomalia, *Langmuir* **2000**, *16*, 15.
[15] H. Nakao, H. Shiigi, Y. Yamamoto, S. Tokonami, T. Nagaoka, S. Sugiyama, T. Ohtani, *Nano Lett.* **2003**, *3*, 1391.
[16] A. Khanal, Y. Inoue, M. Yada, K. Nakashima, *J. Am. Chem. Soc.* **2007**, *129*, 1534.
[17] J. Yuan, Y. Xu, A. Walther, S. Bolisetty, M. Schumacher, H. Schmalz, M. Ballauff, A. H. E. Muller, *Nat. Mater.* **2008**, *7*, 718.
[18] J. Qian, G. Guerin, Y. Lu, G. Cambridge, I. Manners, M. A. Winnik, *Angew. Chem.* **2011**, *123*, 1660; *Angew. Chem. Int. Ed.* **2011**, *50*, 1622.
[19] Y.-Y. Won, H. T. Davis, F. S. Bates, *Science* **1999**, *283*, 960.

